

# Synthesis and Properties of Electrochemically Deposited Vertical Mesoporous Silica Thin Films

Yuan Zhou<sup>1,4</sup>, Qiming Liu<sup>1,3</sup>, Ye Feng<sup>2</sup> and Min Tan<sup>1</sup>

<sup>1</sup>School of Physics and Technology, Key Laboratory of Artificial Micro- and Nano-structures of Ministry of Education, Wuhan University, Wuhan 430072, China

<sup>2</sup>State Key Laboratory of Silicate Materials for Architectures, Wuhan University of Technology, Wuhan 430070, China

<sup>3</sup>College of Chemistry and Materials Science, Hubei Engineering University, Xiaogan 43200, China

<sup>4</sup>GuoDian Science and Technology Research Institute, Nanjing 210031, China

Received: May 25, 2015, Accepted: July 25, 2015, Available online: September 30, 2015

**Abstract:** Electrochemical deposition was successfully used to prepare mesoporous silica thin films with highly ordered and vertically oriented pores. Tetraethyl orthosilicate was used as the inorganic silicon source and cetyltrimethyl ammonium bromide was the template. A negative potential was applied to the working electrode, which was initially immersed in collosol and then in hydroxyl at the electrode/solution interface. Hydroxyl ion served as the catalyst that promoted the polycondensation and self-assembly of the silicon precursor, as well as the formation of thin films with pores which are highly ordered and vertically oriented with respect to the panel. The pore arrangement of the mesoporous film was hexagonal, and its aperture was 2 nm to 3 nm. The verticality of the thin film pore was demonstrated through permeability and transmission electron microscopy analyses. The prepared mesoporous film possessed good optical amorphous antireflective property with ordered and vertically oriented pores.

**Keywords:** mesoporous silica thin film, electrochemical deposition, vertically oriented pores

## 1. INTRODUCTION

Nanostructured mesoporous materials rapidly gained popularity in the 1970s because of their notable features, such as uniform pore size, ordered arrangement and adjustable aperture[1]. Given that mesoporous materials have high specific surface area and superior thermal and hydrothermal stability, they can be applied in adsorption, separation[2], catalysis[3], and loading. Mesoporous materials can also be applied in various fields, such as chemistry, optoelectronics, electromagnetism, ecology and materials science.

Mesoporous material was first regarded as a by-product of cellular material treatment with an unordered aperture. In 1992, Kresge et al.[4]. used self-assembling nano-techniques that involve the use of quaternary ammonium salt cationic surface active agent cetyltrimethyl ammonium bromide (CTAB) as template to prepare mesoporous material MCM-41 with hexagonally ordered arrangement, uniform pores, and adjustable aperture.

Significant effort has been exerted in the preparation of mesoporous thin film materials with pores that are vertical to the substrate surface. Nucleation and directed self-assembly processes are controlled by chemical modification of the solid-liquid interface. However, previous studies have shown that it is difficult to prepare mesoporous film with vertical pores. The present study aimed to synthesize mesoporous thin films on conductive substrate through electrochemical deposition method.

## 2. EXPERIMENTAL

### 2.1. Preparation of mesoporous thin films through electrochemical deposition

The collosol solution for the electrochemical deposition was prepared. CTAB was used as the template and tetraethoxysilane (TEOS) was the inorganic silicon source. Inorganic salt was added to increase electrical conductivity, and the pH of the mixture was regulated to the appropriate level. Through potentiostatic method, voltage was applied to the negative electrode to prepare mesopo-

\*To whom correspondence should be addressed: Email: qmliu@whu.edu.cn

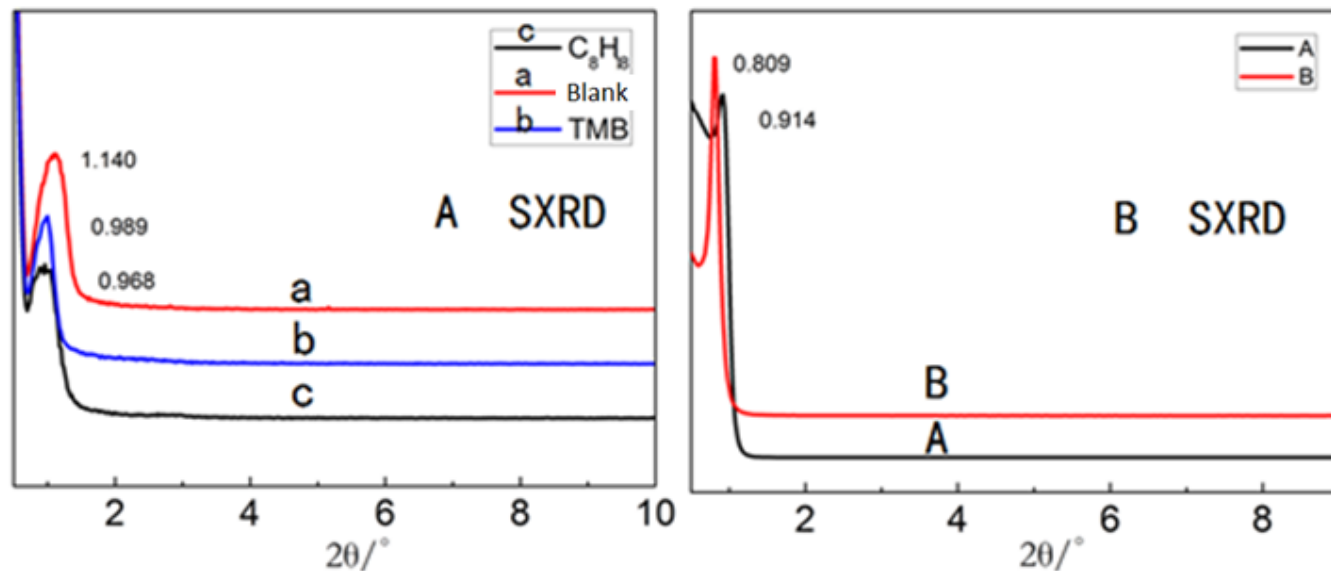


Figure 1. Infrared spectra of the mesoporous thin films. Sample *A*: with template; Sample *B*: without template at 450 °C; Sample *C*: without template in solution.

rous silica film materials with the desired characteristics.

## 2.2. Characterization

The effects of synthesis conditions and other factors on morphology, structure, permeability, and anti-reflection of mesoporous thin films were determined through transmission electron microscopy (TEM), Fourier transform infrared spectroscopy (FTIR); ultraviolet-visible spectroscopy, small-angle X-ray diffraction (XRD), scanning electron microscopy (SEM), and cyclic voltammetry (CV) measurements (CV).

## 3. RESULTS AND DISCUSSION

### 3.1. Infrared analysis of the mesoporous SiO<sub>2</sub> thin film

Fig. 1 shows the infrared spectra of the SiO<sub>2</sub> mesoporous thin films. In the experimental measurements, SiO<sub>2</sub> thin film with a hole structure was obtained. The template was removed and the sample was prepared through electrochemical method. A sample was aged in an oven at 130 °C for 12 h to obtain sample *A*. Another sample was calcined in a muffle furnace at 450 °C for 0.5 h at 2 °C/min heating rate to obtain sample *B*. Another sample was soaked in 0.1 mol/L hydrochloric acid-ethanol solution for 5 min and adequately stirred to obtain sample *C*. Apparent absorption peaks at 2923 and 2852 cm<sup>-1</sup> were observed in sample *A*. These peaks, which were not seen in samples *B* and *C*, were attributed to the stretching vibration peaks of -CH<sub>3</sub> and -CH<sub>2</sub>- in CTAB[5]. The results indicate that both calcination and solvent methods are capable of removing CTAB. The absorption peaks of samples *B* and *C* at 3434 and 3342 cm<sup>-1</sup>[6], respectively, were induced by the hydroxyl vibration of the sample or the hydrogen bonding in the silanol group. The peaks near 1643 cm<sup>-1</sup> of *B* and 1635 cm<sup>-1</sup> of *C* were the remaining water absorption peaks. Samples *A*, *B*, and *C* exhibited absorption peaks near 1228 and 1097 cm<sup>-1</sup>, which corre-

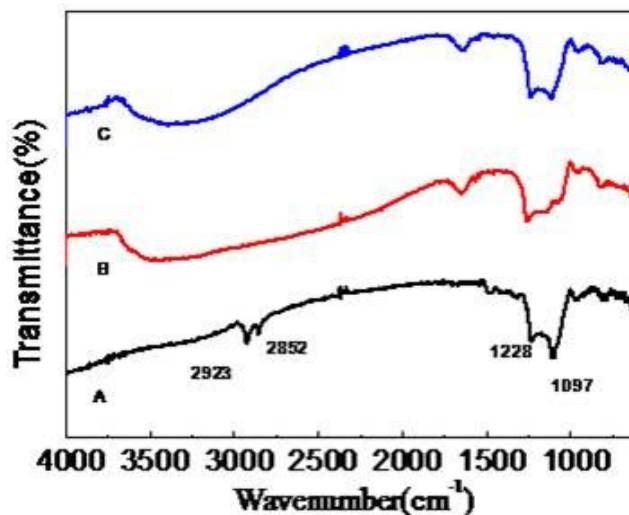


Figure 2. Small-angle and wide-angle XRD patterns of the mesoporous thin films.

spond to Si-O-Si asymmetric symmetrical stretching vibration peak. The three samples also showed peaks near 794 cm<sup>-1</sup>, which represent the Si-O-Si symmetric symmetrical stretching vibration peaks. Therefore, based on the Si-O-Si observed in Fig. 1, the formation of the silicon-based thin-film and the methods, namely, high-temperature calcination at 450 °C and soaking in 0.1 mol/L hydrochloric acid-ethanol solution, can completely remove the CTAB template.

### 3.2. XRD analysis of the mesoporous SiO<sub>2</sub> thin films

As shown in Fig. 2, samples *A* and *B* are small-angle and wide-

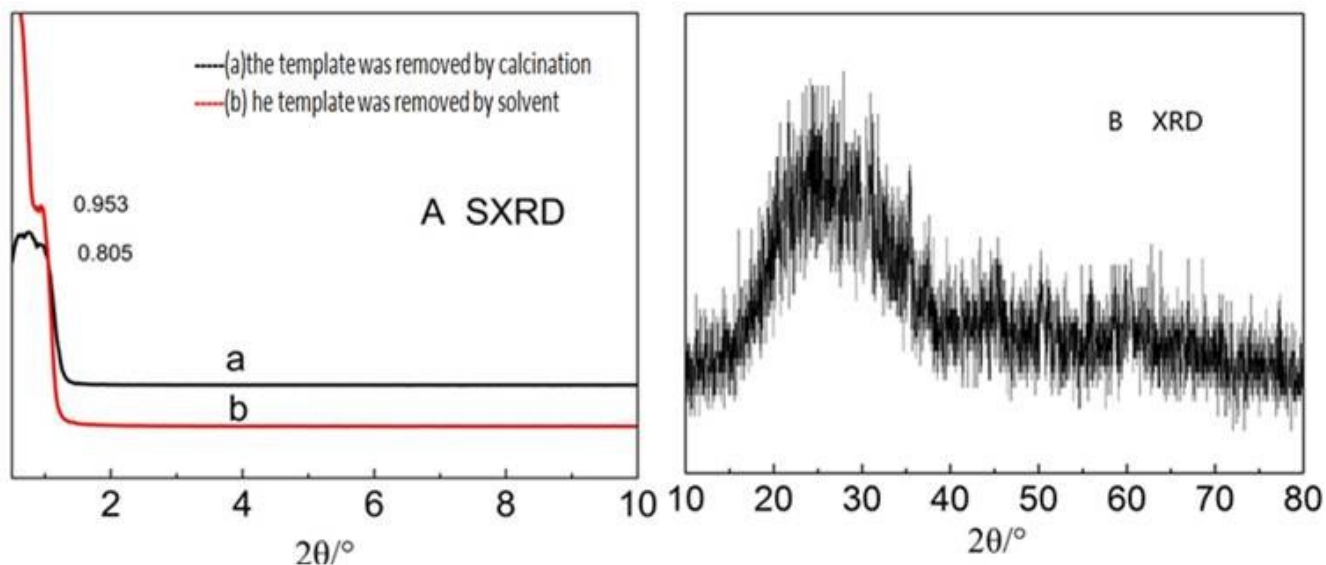


Figure 3. TEM images of the mesoporous thin films.

angle XRD patterns, respectively. Fig. 2A shows that the template was removed through calcination and solvent methods. Only one peak ( $2\theta$  at 0.953) was observed in the calcination method. The removal of CTAB was also demonstrated by the formation of mesoporous holes (Fig. 3). Only one peak was found in the small-angle XRD pattern, indicating that the thin film did not have a long-range ordered structure. After the removal of CTAB through solvent method, the same peak was observed. Based on the TEM image, this long-range non-ordered structure was due to the overlapping arrangement of the thin film hole or the deformation and displacement of the hole grid[7]. Fig. 2B is the  $10^\circ$  to  $80^\circ$  wide-angle XRD pattern of the mesoporous silica thin film. A relatively wide and weak diffraction peak at approximately  $27^\circ$  was found, confirming that the mesoporous thin film is non-crystalline. Therefore, the removal of the CTAB template resulted in a short-range ordered arrangement of the pores and a random amorphous thin film framework structure.

### 3.3. TEM analysis of the mesoporous SiO<sub>2</sub> thin films

Mesoporous pores were observed in the TEM image of the thin films (Fig. 3A). The relatively ordered section A is discussed separately. Fig. 3 shows the top-view TEM images of samples B, C, and D, which correspond to fast FTIR patterns marked by red lines. E shows the FTIR pattern of the entire sample.

When electron beam is used to irradiate crystal sample, an electron diffraction pattern can be obtained on the fluorescent screen of the back focal plane of the objective. Several similarities exist between electron diffraction and X-ray diffraction. Mesoporous SiO<sub>2</sub> thin film is amorphous, but it has regular and ordered pore arrangement. Few recognizable peaks are found on its XRD pattern. This phenomenon is due to the numerous defects of the pore structure of the mesoporous material, and many irregularly arranged pores have

lower diffraction capability. The same phenomenon does not occur with the use of TEM. Given that the scattering factor of the interaction between the electron beam and the sample is 104 times that of the interaction between the X-ray and the sample, the electron diffraction pattern can be easily distinguished from the TEM fluorescent screen. Some diffraction beams can be used as new incident beams to generate continuous secondary Bragg diffraction or multiple Bragg diffractions because the strength of crystal diffraction beam is similar to that of TEM. Primary and secondary diffraction spots generated by the diffraction overlap to change the spot strength. Diffraction spots that are not overlapped cause the emergence of diffraction spots on electron diffraction patterns, which normally have zero structure and are extinct. Given that the mesoporous material sample is thick and easily generates the effect of secondary diffraction or multiple diffractions. Determining the extinct law of the sample from the electron diffraction pattern is sometimes impossible. Thus, FTIR is used.

The diffraction piebald of section B (Fig. 3) is an incompletely closed ring with several bright dots. This section is the boundary location of the hole structure in a different orientation. During electrochemical deposition, uniform distribution of ampere density is difficult, which leads to different densities of the thin film under various internal stresses, thereby forming such disordered boundary. The diffraction results of the piebald of section B also confirm this result.

In section C, the arrangement of the pores is regular and orderly. The diffraction piebald also shows hexagonal arrangement of the pore structure. Together with the permeability analysis of potassium ferricyanide for the thin film, the results indicate that some pores are fluent. Such structure satisfies the requirement for applications in drug controlled release. The material is transported from the surface of the thin film to the bottom, resulting in mesoporous material with significantly large specific surface area.

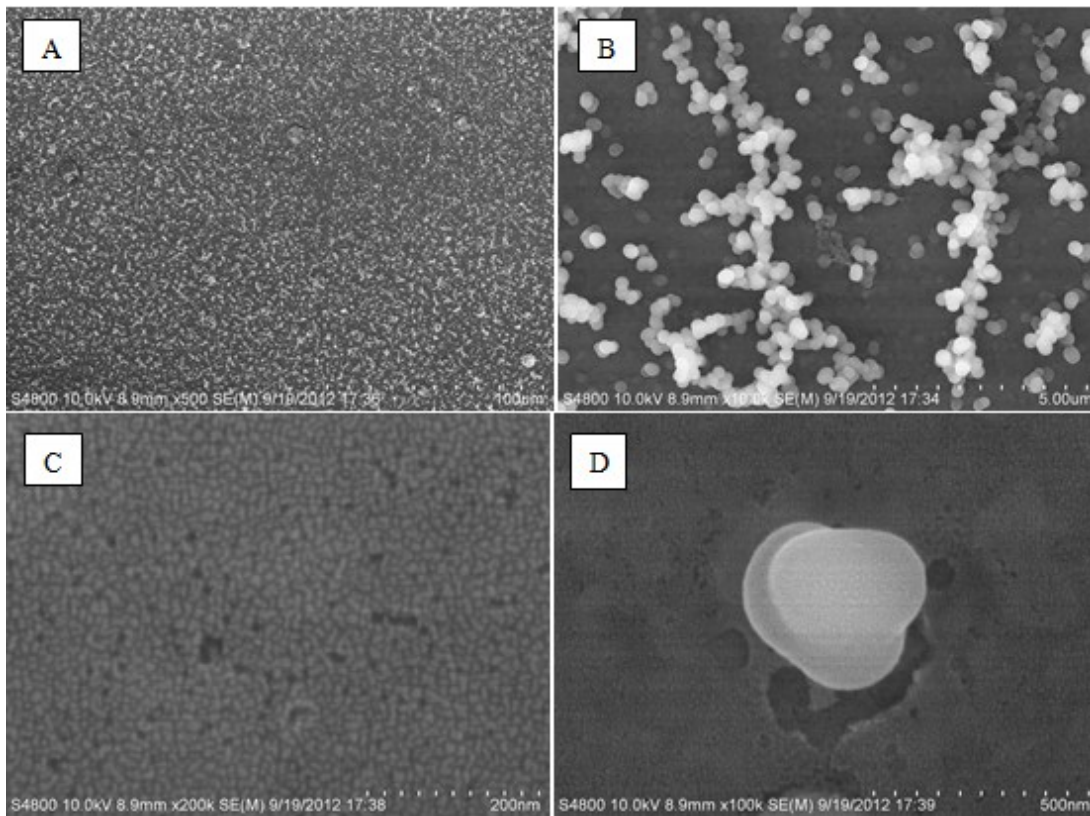


Figure 4. Tangent plane of the TEM test results of the sample.

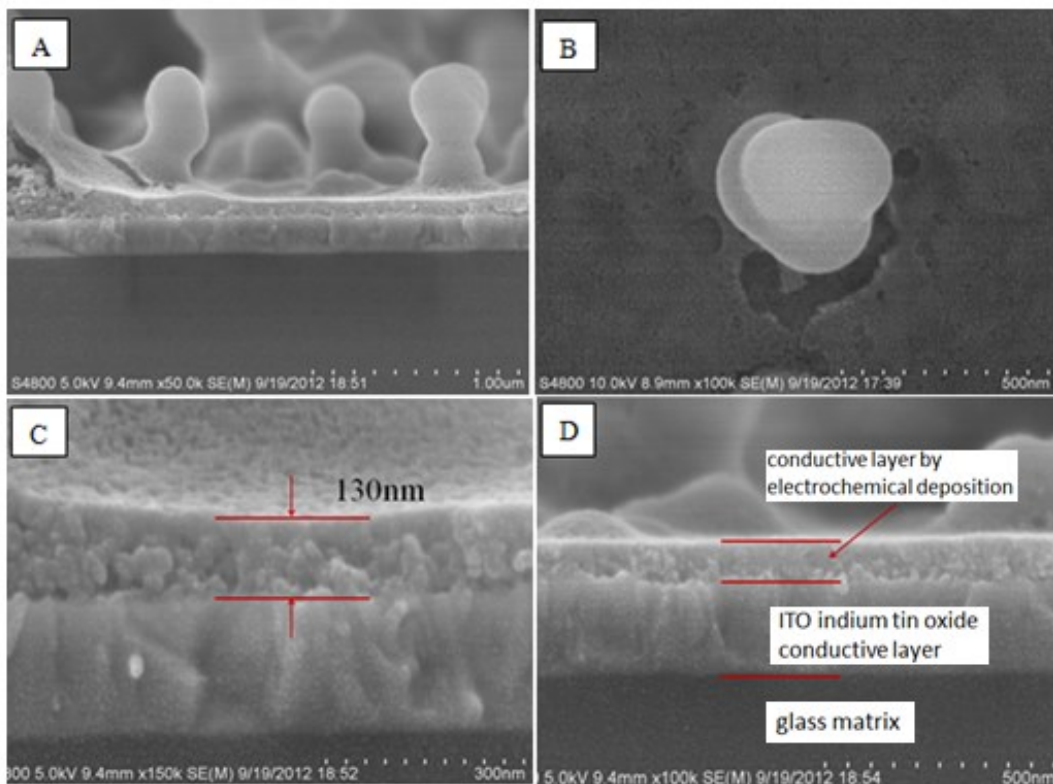


Figure 5. Permeability analysis through CV in potassium ferricyanide solution of the mesoporous thin film.

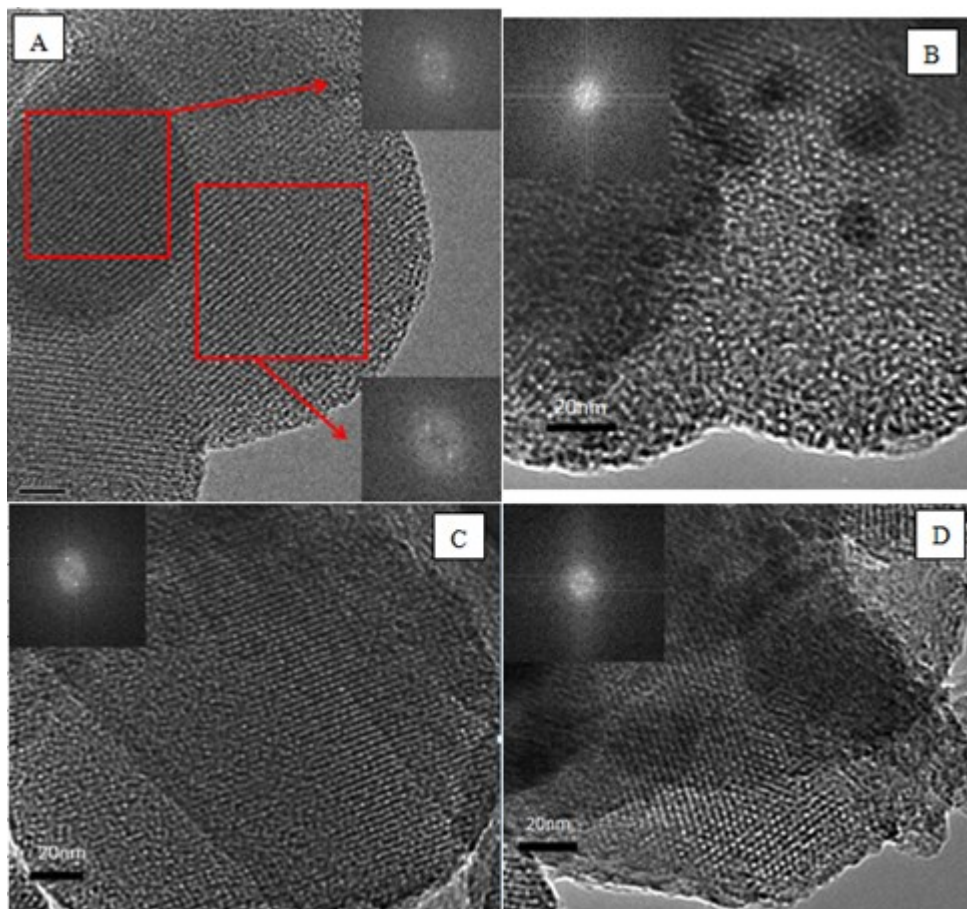


Figure 6. TEM images of the mesoporous thin films

The diffraction piebald of section *D* also indicates the presence of pores with orderly arrangement, but these pores are less bright and have less degree of order compared with those in section *C*. This observation could be due to the differences in ampere density caused by the working electrode during electrochemical deposition. Moreover, under an electric field, CTAB templates of directional alignment are not identical. The degree of hydrolytic polycondensation of ethyl silicate TEOS around the micelles can also cause a difference in the ampere density. All of these factors increase the difficulty in preparation of thin-film mesoporous silica with long-range order and good homogeneity.

Some of the FTIR piebald were elliptical, suggesting the inhomogeneity of the hole lattice deformation. The hexagonal structure in the ellipse also underwent particular deformation, indicating the existence of different stresses in the major and minor axis. Therefore, stress was applied to both the inclined boundary in the small-angle and wide-angle XRD patterns. Given that the major axis was slightly affected, the boundary interface of the minor axis expanded in the inclusive interface of the crystal lattice. Consequently, the aperture of this section was less than the other pores during mesoporous material formation. The crystal boundary sections experienced concentrated stress, which caused deviation from the expected ordered structure[8].

The pores near the boundary were not damaged; they were just

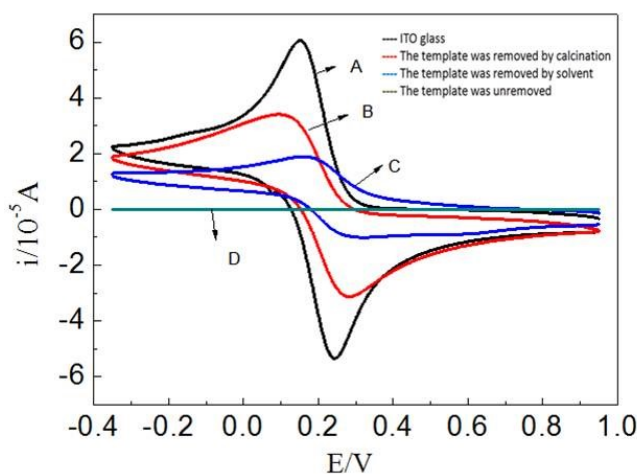


Figure 7. Cyclic voltammetry graph of mesoporous thin films in potassium ferricyanide solution for permeability analysis; a: CV curve for the ITO conductive glass, b: CV curve for the calcination removing template agent, c: CV curve for the solvent removing template agent, d: CV curve not removing the template agent

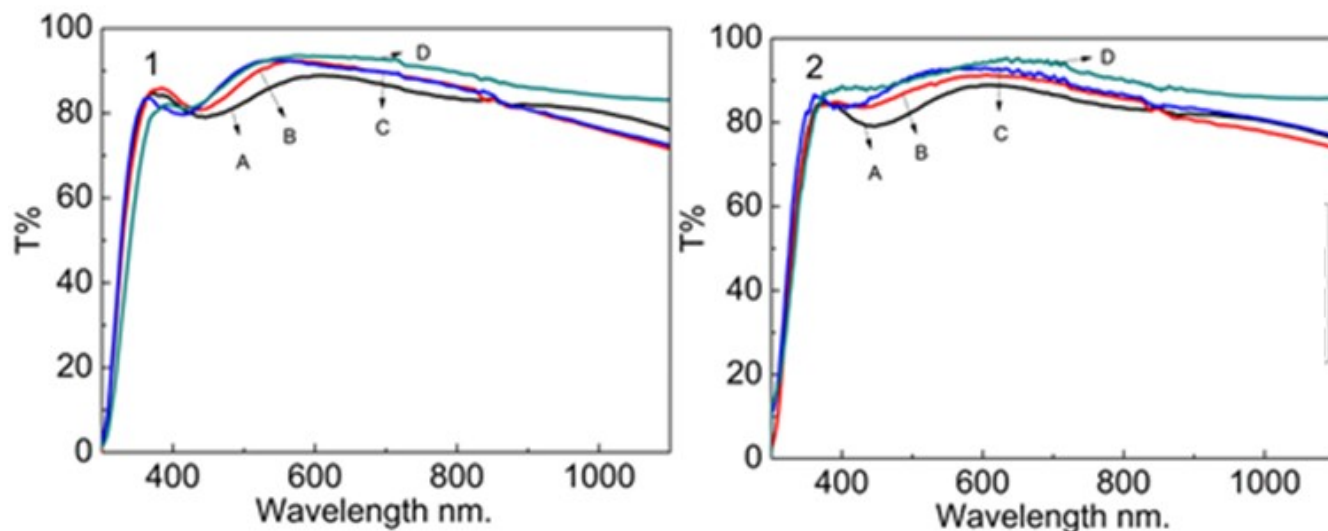


Figure 8. Transmission curves of mesoporous thin films; 1: without expanding agent, 2: with expanding agent, A: The blank sample, B: Not removing the template agent, C: The solvent removing template agent, D: The calcination removing template agent

rotated, displaced, and inclined, confirming the stability of the mesostructured material. The transverse section plane of the mesostructured thin film shows that short pores were normally straight. Even the pores of the defect area bearing the internal stress were hardly bent or twisted. This characteristic indicates the mechanical strength of the material.

Fig. 4A shows the tangent plane of the mesoporous thin film of the template removed using 0.1 mol/L hydrochloric acid–ethanol solution. The template in Fig. 4B is removed by calcination at 450 °C for 30 min at 2 °C/min increase rate. The two TEM images and their respective FTIR piebald confirm the formation of pores of mesoporous material (2D hexagonal structure). Figs. 4A and 4B show the pores of the mesoporous thin film. The width of the white area in *B* is larger than that of *A* due to the shrinking of the duct and wall of the mesoporous structure during calcination under high temperature, resulting in uncertain aperture reduction. The aperture in *A* is approximately 3.3 nm and that in *B* is only 2.8 nm, indicating that *B* shrinks more. Varying ampere densities result in rotation, displacement, and inclination of pores of the mesoporous material. The transverse section plane *A* of the mesostructure thin film demonstrates that pores normally maintain straight arrangement; even the pores of the defect area bearing the internal stress hardly bend or twist. However, the lower left part of pores in *B* is displaced, thereby affecting the transmission of pores.

Curve *A* is the CV of indium tin oxide (ITO) conductive glass, curve *B* is the CV of the sample with its template removed by calcination, curve *C* is the CV of the sample with its template removed by dissolution, and curve *D* is the CV of the sample with intact template.

The permeability analysis test conducted through CV of the mesoporous thin film in potassium ferricyanide solution demonstrates the permeability of the pores (Fig. 5)[9]. The electrolyte solution used was a mixture of 0.5 mmol/L KCl solution of  $K_3Fe(CN)_6$  and 0.1 mmol/L KCl. Detailed information on the penetrating quality of the mesoporous thin film were obtained through CV.  $K_3Fe(CN)_6$  is

a reduction–oxidation (redox) detector that elicits a response if the probe reaches to the surface of the electrode by diffusion[10]. As seen in the CV (curve *A*) of the ITO conductive glass, the probe reached the surface of electrode ITO without any obstruction, resulting in high redox peak. Curve *B* shows the CV curve of the silica mesoporous thin film, the template of which was removed via calcination for 30 min at 450 °C and then plated on the ITO conductive glass. The position of the redox peak decreased, indicating that the electronic probe  $Fe^{3+}$  was impeded by the thin film while traveling to the ITO surface for the commencement of the redox reaction. The  $Fe^{3+}$  probe can only reach the surface through the mesoporous channel. Thus, the silica mesoporous pores prepared through electrochemical deposition indirectly confirmed the permeability of the material and the vertical arrangement of the pores with respect to the ITO conductive glass surface. This arrangement favors the selective transfer of the material from the film surface to the ITO surface, a characteristic which may have a number of potential applications. Curve *C* is the CV of the sample whose template was removed via solution extraction method[11] (soaking and stirring in 0.1 mol/L hydrochloric acid–ethanol solution for 5 min). The redox reaction resulted in decreased peak height, suggesting that the mesoporous film pores whose template was removed exhibited permeability. However, the peak declined compared with that in curve *B*. The template of the FTIR spectrogram surface (Fig. 1) was completely removed, indicating that such phenomenon may not be due to the removal of the template, but rather the Si–OH bonds in the pores that affect  $Fe^{3+}$ [12]. The specific reasons for this phenomenon are unclear and require further study. Curve *D* is the CV of the sample whose template was not removed. Compared with curves *A*, *B*, and *C*, the thin film with intact template was not permeable and did not crack.

#### 4. CONCLUSIONS

In this study, mesoporous thin films with ordered arrangement and vertically oriented pores were successfully prepared through

electrochemical deposition.

The FTIR spectra indicated that solvent extraction and high-temperature calcination can effectively remove the template. The SEM images showed that the depositional mesoporous thin film was uniformly distributed at the surface of the ITO glass substrate and the thickness of the thin film was approximately 110 nm. The lateral view of the film also demonstrated this phenomenon, which was significantly altered by the high-temperature processing of the thin film hole wall. Small-angle XRD pattern of the thin film exhibited the presence of diffraction peaks at small angles, indicating the formation of the thin film pores. The small-angle peak in the pattern of the sample obtained through calcination was higher than that of the sample extracted through solvent method. In addition, high temperature released stress and increased the order of the thin film structure.. CV tests for mesoporous thin film using potassium ferricyanide showed that the permeability of the mesoporous thin film pores was good, indirectly demonstrating their vertical alignment to the ITO glass.

## **5. ACKNOWLEDGEMENTS**

This research work was financially supported by the National Natural Science Foundation of China (51272183), The Hubei Provincial Natural Science Foundation (2012FFA042), and the self-determined and innovative research funds of Wuhan University.

## **REFERENCES**

- [1] C T Kresge, M E Leonowicz et al., *Nature*, 359, 710 (1992).
- [2] Adhyapak P.V., Karandikar P., Vijayamohan K., *Mater. Lett.*, 58, 1168 (2004).
- [3] Bore M.T., Pham H.N., Switzer E., *J. Phys. Chore. B*, 109, 2873 (2005).
- [4] Sivakumar Nagarajan, Mingqi Li, et al., *Adv. Mater.*, 20, 246 (2008).
- [5] Bagshaw S.A., Pinnavaia T.J., *Science*, 269, 1242 (1995).
- [6] Shunsuke T., Hiromi T., Takanori M. et al., *Thin Solid Films*, 495, 186 (2006).
- [7] Yang H., Coombs N., Sokolov I. et al., *Nature*, 381, 589 (1996).
- [8] Fang-Fang Xu, Fang-Ming Cui, Mei-Ling Ruan, Lin-Lin Zhang and Jian-Lin Shi, *Langmuir*, 26, 7535 (2010).
- [9] Aure' lie Goux, Jaafar Ghanbaja, Alain Walcarius Prussian, *J. Mater. Sci.*, 44, 6601 (2009).
- [10]Stephanie Sayen, Alain Walcarius, *Electrochemistry Communications*, 5, 341 (2003).
- [11]Yann G., Mathieu E. et al., *J. Mater. Chem.*, 20, 6799 (2010).
- [12] Tanev P.T., Pinnavaia T.J., *Science*, 267, 865 (1995).